

Mechanical Properties of Plasma-Hardened 5% Chromium Tool Steel Deposited by Arc Welding

Plasma heat treatment promotes an increase in mechanical properties of deposited metal

BY L. K. LESHCHINSKIY AND S. S. SAMOTUGIN

ABSTRACT. A complex technology is proposed to increase the mechanical properties of tools, dies and machine components for hot work of metals. The combination of hardfacing with a 5% chromium deposited metal and subsequent surface treatment using a highly concentrated plasma jet creates a hard surface along with resistance to breakage upon impact. The extremely fine-grained martensite structure and relevant property gradients of the plasma-jet-hardened layer are almost identical to those treated by laser and electron beams.

Due to rapid phase recrystallization, the dissolution of primary carbides and the saturation of a solid solution with carbon and alloying elements develop. This leads to an increase in the degree of tetragonality, microdistortions of the crystal structure and to an increase in hardness without a decrease in dynamic fracture toughness because of the high dislocation density and mosaic block size reduction.

In its mechanical properties, martensitic 5% chromium (0.20% C) deposited metal after plasma hardening is close to chromium hot-work die steels, significantly surpassing them in dynamic fracture toughness.

Introduction

Hardfacing has traditionally been used to increase the performance of machine components, tools and spare parts. Through the proper selection of a hardfacing alloy and process, there is the possibility of achieving high service properties and of reducing the consumption of metal. For hardfacing of tools, dies and machine components used for hot deformation of metal, 5% chromium tool steel [5 Cr-0.5 Mo-0.15 V (0.20 C)] is widely used (Refs. 1, 2), but when compared to

hot-work die steels, it needs improvement in mechanical properties and wear resistance.

A promising method for improving hardness and wear resistance, without the additional alloying of deposited metal, is a surface heat treatment using a highly concentrated heat source. The surface heat treatment of metals by a highly concentrated plasma jet similar to the heat sources used more extensively — laser and electron beams — makes it possible to carry out the power density 10^4 – 10^5 W/cm². Although not many experimental data reports are available on plasma hardening, experience with the application of plasma hardening indicates the cooling rates of the surface layers of steels, their structure and hardness are almost identical to those of the same materials hardened by laser and electron beams (Refs. 1, 3–5).

Recent studies of plasma surface treatment have shown high compressive residual stresses are formed in the quenched layer. These stresses rapidly decrease at the boundary of the quenched layer, change their sign and transfer to tensile stresses. The nonuniform distribution of the residual stresses in the depth of the heat-affected zone (HAZ) has a positive effect on the fracture toughness of hardened steels: cracks, caused by the external cooling, cease to grow at the boundary of the quenched layer.

According to the high cooling rates and quenched structure in the HAZ of

5% chromium deposited metal, reduction in impact strength and dynamic fracture toughness can be expected. This paper describes a study conducted to investigate the mechanical properties of plasma-hardened deposited metal. Experiments are described and discussed using a comparison of microstructures, fractographic pictures, X-ray diffraction studies and mechanical tests of deposited metal in the initial state and after plasma surface hardening. The theoretical analysis is also presented.

Experimental Procedure

Following multipass surfacing of 5 Cr-0.5 Mo-0.15 V (0.20 C) metal using the submerged arc welding process (Ref. 6), 10 x 10 x 55 mm Charpy specimens were sectioned, mounted and plasma hardened across one of the lateral faces — Fig. 1A. The specimens were machine finished, including notching of the very sharp, narrow notch in the middle of HAZ — Fig. 1B. The sharpness of the notch tip promoted early crack initiation in the Charpy test; therefore, it simulated a natural crack well enough to provide a valid dynamic fracture toughness K_I test result (Refs. 7, 8). The tests were conducted at 20°C and ten specimens were tested for each structural constitution. When the Charpy test of each specimen was completed, its shape after fracture was checked to be sure the specimen was fractured in the plane-strain fracture toughness test.

The determination of K_I based on Charpy impact tests requires proof the specimen size used is satisfactory. The correlation criterion (Refs. 7, 8) pertains to a Charpy precracked specimen thickness of $B \geq 2.5 (K_I / \sigma_y)^2$. For 5 Cr-0.5 Mo-0.15 V (0.20 C) deposited metal, $K_I = 30$ MPa m^{1/2}, $\sigma_y = 900$ MPa is the yield strength in tension. The calculation determines that when the left-hand member B is equal to 10 mm, it is about ten times greater than the right-hand member of this inequality.

KEY WORDS

5% Chromium Tool Steel
Surfacing/Hardfacing
Concentrated Heat Source
Plasma Surface Hardening
Heat-Affected Zone
Mechanical Properties
Fracture

L. K. LESHCHINSKIY was formerly with Azov State Technical University, Mariupol, Ukraine. S. S. SAMOTUGIN is with Azov State Technical University, Mariupol, Ukraine.

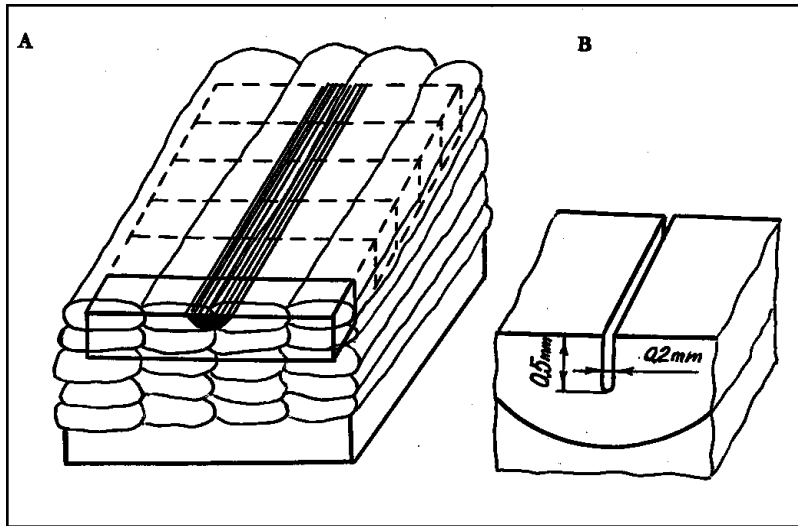


Fig. 1 — Multipass deposited metal sectioned into specimens for notch bar impact testing (A) and forming of the notch in the specimens (B).

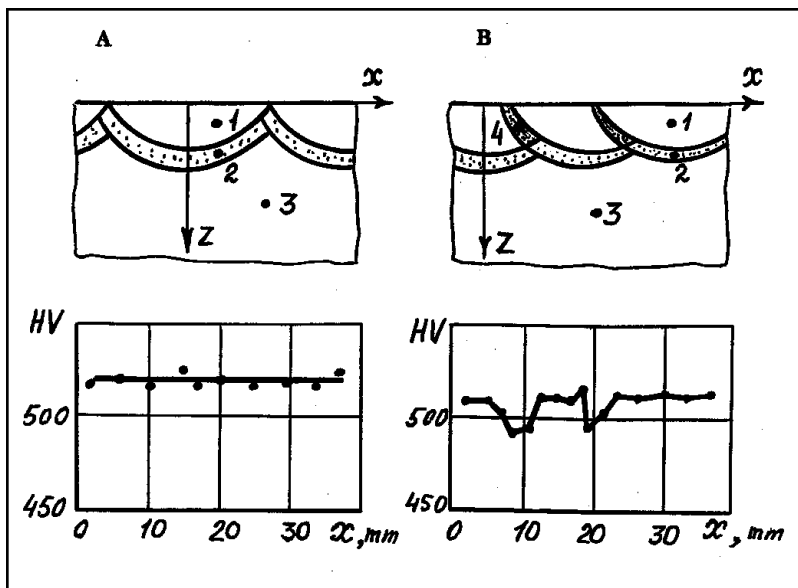


Fig. 2 — Cross section of the HAZ of plasma hardening and distribution of the hardness at the surface ($Z = 0$) of the deposited metal 5 Cr-0.5 Mo-0.15 V (0.20 C). A — Without overlapping of the HAZ; B — with 30% overlap.

Following impact tests, fractured surfaces were analyzed with a scanning electron microscope. Polished and etched sections were examined using an optical metallograph at magnification up to 550X. Thin foil electron micrographs were obtained at different magnifications to further analyze the structure of different regions of the HAZ. The carbide content was determined from the ratio of the masses of deposit precipitated during electrolytic distribution and the dissolved part of the specimen. Phase constitution and crystal lattice parameters in specimens of deposited metal in an initial state

and after plasma hardening were determined using an X-ray diffractometer (Refs. 9, 10) (see Appendix).

Standard metallurgical procedures were used to prepare samples for hardness studies. A Vickers indenter with a 100-g load was used to measure hardness along the different regions of the HAZ and the unaffected deposited metal. The wear testing configuration included unidirectional metal/metal sliding with an oil-abrasive interlayer between the surfaces. This is related to the wear testing configuration listed by the American Society for Lubrication Engineers (Ref. 8).

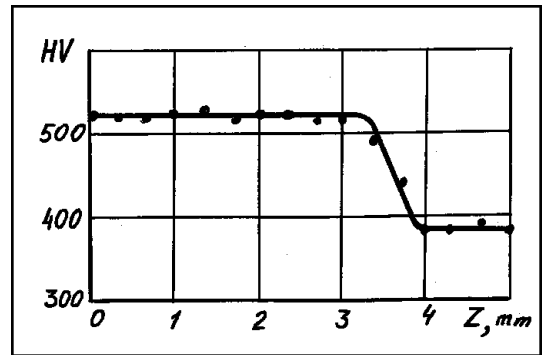


Fig. 3 — Hardness profile of 5% chromium deposited metal quenched with a plasma jet.

Results and Discussion

A single pass of the plasma jet with extremely high heating and cooling rates forms a heat-affected zone of a circular segment with the maximum depth (up to 5 mm) in the center and gradual reduction of the depth to zero when approaching the edge (the width is up to 20 mm) (Refs. 1, 3-5). Table 1 shows the calculated values of the heating temperature and cooling rates in the HAZ of deposited metal 5 Cr-0.5 Mo-0.15 V (0.20 C) for distinct values of arc current I , travel speed of the torch V and plasma gas restriction orifice D of the plasma jet with a power of 30 kW generated by a non-transferred plasma torch with a sectional interelectrode insert. Calculated data were determined for the model of heating of a semi-infinite body by the Gaussian power density distribution of the moving heat source. Plasma surface hardening is carried out without HAZ overlapping (Fig. 2A) as well as with HAZ overlapping — Fig. 2B. The advantage of treatment without HAZ overlapping is the formation of a hardened layer with more uniform hardness and higher wear resistance on the surface when compared to the treatment with HAZ overlapping. At the same time, however, in the latter case, the depth of the hardened layer is more stable.

The structure of the HAZ of a plasma jet single-pass hardened surface is inhomogeneous. The quenched zone (marked 1 in Fig. 2) is placed directly below the hardened surface, where the rapidly increasing temperature is higher than Ac_3 . By increasing the distance to the surface, the transition region of the incomplete quenched structure (marked 2 in Fig. 2) develops according to the heating temperature range Ac_3 - Ac_1 . Below this zone, the metal of the initial structure remains unchanged (marked 3 in Fig. 2). The hardness values obtained in the quenching zone are relatively constant

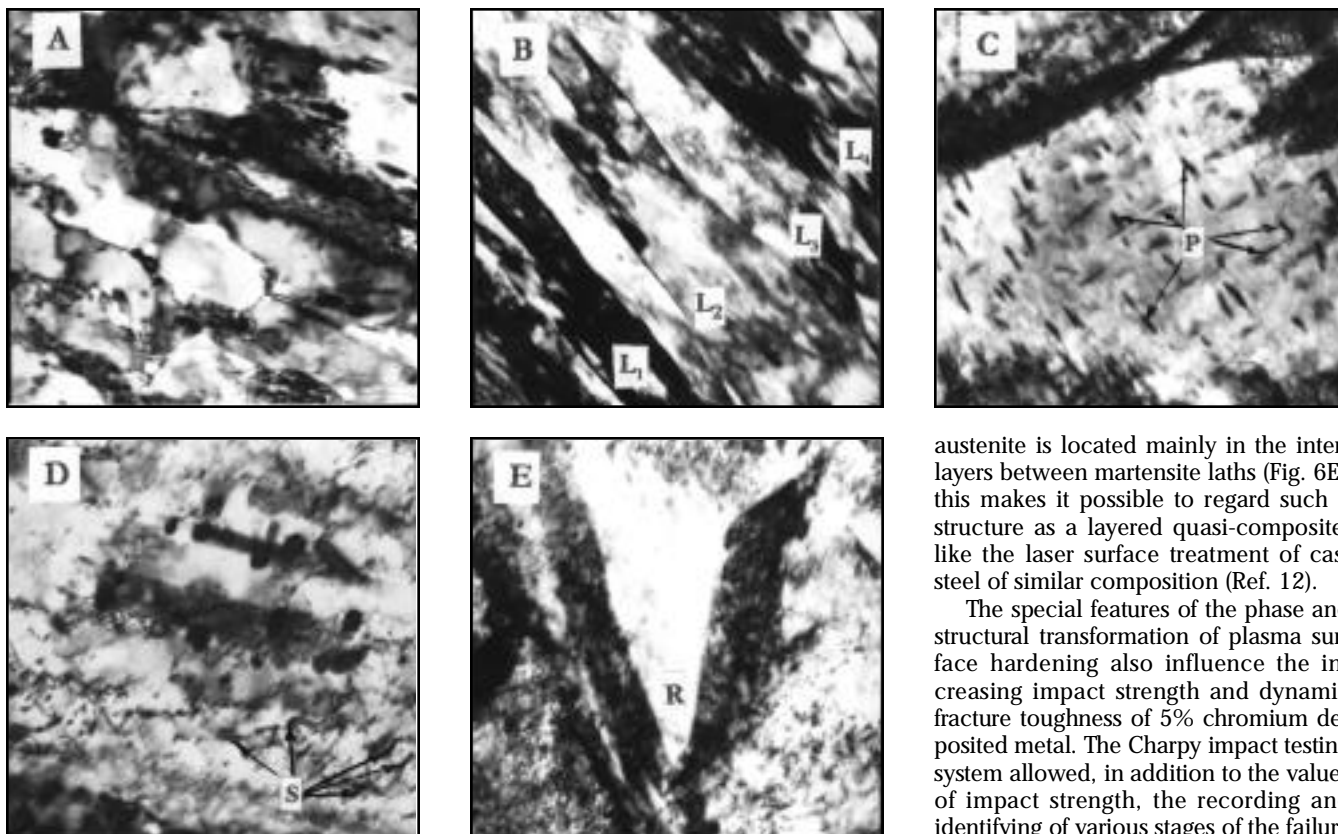


Fig. 6 — Electron micrographs of the structure of the 5 Cr-0.5 Mo-0.15 V (0.20 C) deposited metal. A — In the initial state (22,000X); B — martensite laths (marked L1 to L4) (18,000X); C — carbide phase in martensite (marked P) (32,000X); D — dislocations in martensite (marked S) (52,000X); E — retained austenite (marked R) and martensite (32,000X). B through E are after plasma hardening.

for steels of the same type of composition (Ref. 12, 13), as well as for plasma hardening of tool steels (Ref. 14, 15).

The retardation of martensite self-tempering during rapid hardening is caused by inhomogeneity of carbon distribution in γ -solid solution, which is inherited from austenite in the areas of increased carbon content (related to the average carbon content in the initial state of deposited metal). These areas are more stable against the decomposition. Another confirmation of the retardation in self-tempering and the concentrated inhomogeneity of martensite is the appearance of a heavily degenerated singlet (002) in the X-ray structure analysis.

Supersaturation of a solid solution with carbon and alloying elements as a result of primary carbide dissolution promotes an increase in hardness of deposited metal and a steep increase in dislocation density with a simultaneous increase in strength and deformation ability. The remaining small special carbides and submicroscopic tertiary carbides in martensite crystals of the quenched zone cannot be regarded as a separate hardening phase, but only as a particular in the stimulation to self-

harden the martensite phase. Therefore, the 5 Cr-0.5 Mo-0.15 V (0.20 C) deposited metal after plasma hardening should be classified as belonging not to the martensite-carbide class but strictly to the martensite class. Finely dispersed martensite can play the role of a matrix, as well as of a strengthening phase. Such a structure of the hardened metal has a higher level of mechanical properties as compared to the initial state — hardness, impact strength, dynamic fracture toughness (Table 2). In addition, heat resistance is increased: hardness around HV 500 remains while the heating temperature is raised up to 550°C. If stress-relief bulk tempering is used after hardfacing before plasma hardening, heat resistance can reach 570°C (Ref. 1).

The increased retained austenite content also promotes the improvement of mechanical properties of the hardened deposited metal, especially of dynamic fracture toughness. The γ -phase in the conditions of high heating and cooling rates, short exposure time during plasma surface treatment and inhomogeneity of the solid solution (diminishing of temperature range M_s – M_d), acquires a very fine-grained structure. Because retained

austenite is located mainly in the interlayers between martensite laths (Fig. 6E), this makes it possible to regard such a structure as a layered quasi-composite, like the laser surface treatment of cast steel of similar composition (Ref. 12).

The special features of the phase and structural transformation of plasma surface hardening also influence the increasing impact strength and dynamic fracture toughness of 5% chromium deposited metal. The Charpy impact testing system allowed, in addition to the values of impact strength, the recording and identifying of various stages of the failure process, while measuring the impact velocity, etc. — Fig. 7. This is especially important when a complicated failure process develops for a specimen of hardened steel with the cross section of an abrupt boundary from the quenched (harder) structure to the initial (softer) structure. The failure process is initiated and extends within the hardened layer. However, at the boundary, it ceases to propagate. To continue the failure process of such a specimen, significantly more Charpy energy is necessary (Fig. 7B) when compared to the energy necessary for the failure of the specimen with a homogeneous structure — Fig. 7A. The data on impact strength (CVN = 48.0 J) and dynamic fracture toughness ($K_{I,d} = 32.5$ MPa m) of the deposited metal after plasma surface hardening show the enhancement as compared to the results of the testing with a similar procedure for the same type of specimens of the bulk-hardened chromium hot-work die steel 5 Cr-1.7 Mo-0.32 V (0.33 C). In the latter case, CVN = 36.0 J and $K_{I,d} = 25.3$ MPa m.

To obtain a better understanding of the failure micromechanism of plasma-hardened 5 Cr-0.5 Mo-0.15 V (0.20 C) deposited metal, a fractographic examination was carried out on the fracture surfaces of impact test specimens. The failure micromechanism of the deposited metal in the initial state is quasi-brittle, a combination of transcrystalline cleavage (dominant) + ductile microvoid coalescence — Fig. 8A. Plasma hardening

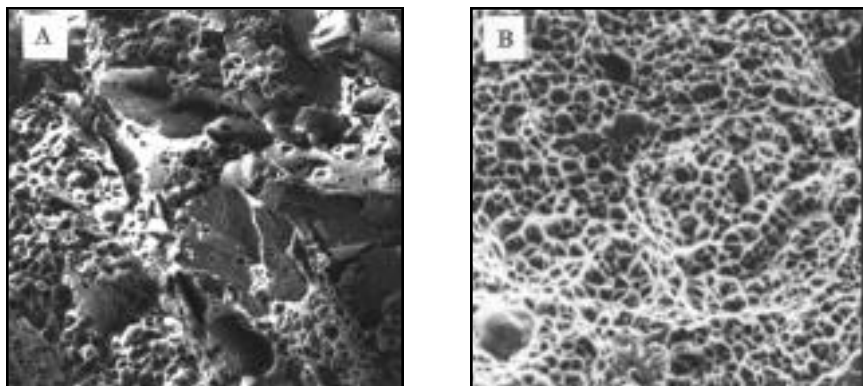


Fig. 8 — Fracture surface from room temperature impact test of specimens of the 5 Cr-0.5 Mo-0.15 V (0.20 C) deposited metal by means of a scanning electron microscope (400X). A — In the initial state; B — after plasma hardening.

Conclusions

The results, based on the investigations, confirm the effect of surface hardening by a highly concentrated plasma jet on the structure and mechanical properties of 5 Cr-0.5 Mo-0.15 V (0.20 C) deposited metal validates the following conclusions:

- The structure of the deposited metal in the initial state is highly tempered lath martensite. The carbide phase is represented by cementite Fe_3C and special carbides $Me_{23}C_6$.
- Plasma heat treatment of the deposited metal leads to full phase recrystallization and rapid quenching with formation of a hardened layer of very finely dispersed martensite structure. Martensite morphology does not change; lath martensite is being formed. Self-tempering of martensite in the plasma quenched zone is stopped at the initial stage and its parameters are practically the same as the original martensite.
- During plasma hardening, the full dissolution of the cementite phase and of the major part of the special carbides takes place, which leads to additional saturation of the solid solution with carbon and alloying elements. As a result, there is an increase in the martensite crystal lattice parameter a , degree of tetragonality c/a and microdistortions of the crystal lattice ϵ . Hardness increases from HV 390–410 to HV 520–540. The sharp rise in dislocation density and mosaic block size reduction S govern the simultaneous rise in hardness, impact strength CVN and dynamic fracture toughness K_{1d} .
- The rise in the dynamic fracture toughness of the plasma-hardened deposited metal is caused by qualitative alteration of the micromechanism of failure from transcrystalline cleavage (Kottrell's dislocation model) to ductile microvoid coalescence (Yokobori's dislocation model).

Acknowledgments

The authors are grateful to V. Goritsky, D. Khromov and E. Zarkhova for EM metallographs, and to N. Solyanik, E. Lokshina, O. Novohatskaya, V. Velgovol'skaya, S. Disenhof and T. Kiritseva for their help in carrying out this work.

References

1. Leshchinskiy, L. K., Samotugin, S. S., Pirch, I. I., and Komar, V. I. 1990. *Plasma Surface Hardening*. Kiev, Tekhnika. pp. 5–9, 45–53.
2. *Materials and Processes*. Third Edition. 1985. Part A: Materials. New York, N.Y., pp. 255–259.
3. Gurarie, V. N. 1984. Hardening in steels subjected to high-velocity intensive plasma treatment. *Metals Forum* 7(1): 12–21.
4. Arata, Y. 1986. *Plasma, Electron and Laser Beam Technology*. ASM International, Materials Park, Ohio, pp. 568–579.
5. *Metals Handbook*. Vol. 4. 1995. Heat Treating. ASM International, Materials Park, Ohio, pp. 291–307.
6. Leshchinskiy, L. K., Samotugin, S. S., Goritsky, V. M., Khromov, D. P., and Zarkhova, E. I. 1996. Structure and crack resistance of 18Cr6MoVMnSi deposited metal after plasma strengthening. *Avtomat. Svarka* 8: 31–35.
7. *Standard Test Methods for Mechanical Testing of Metals. The Determination of the Dynamic Fracture Toughness (Crack Resistance)* RD 50-344-82. 1982. Moscow, USSR, Standards.
8. *Metals Handbook*. Vol. 8. 1995. Mechanical Testing. ASM International, Materials Park, Ohio, pp. 259–268, 601–603.
9. Mirkin, L. I. 1976. *X-ray Structural Analysis*. Moscow, Nauka, pp. 135–149.
10. Vasilev, D.M. 1977. *Diffraction Methods in Structural Analysis*. Moscow, Metallurgiya, pp. 67–78.
11. Kurdjumov, G. V., Utevskiy, L. M., and Entin, R. I. 1977. *Transformations in Iron and Steel*. Moscow, Nauka, pp. 58–69, 105–114.

12. Molian, P. A. 1985. Structure and hardness of laser-processed Fe-0.2% C-5% Cr and Fe-0.2% C-10% Cr alloys. *Journal of Material Science* 20: 2903–2912.

13. Molian, P. A. 1986. Engineering applications and analysis of hardening data for laser heat treated ferrous alloys. *Surface Engineering* 2(1): 19–28.

14. Leshchinskiy, L. K., et al. 1985. Structure and properties of deposited metal on carbon steels hardened with a plasma jet. *Welding Production* 32(11): 34–36.

15. Samotugin, S. S. 1998. Plasma treatment of tool steels. *Welding International* 12(3): 225–228.

16. Hellan, K. 1984. *Introduction to Fracture Mechanics*. New York, N.Y., McGraw-Hill, pp. 142–153.

17. Yokobori, T. 1968. *An Interdisciplinary Approach to Fracture and Strength of Solids*. Groningen, Wolters-Noordhoff Scientific Publications, pp. 123–157.

Appendix: The Determination of Phase Constitution and Crystal Structure Parameters

The crystal structure of 5 Cr-0.5 Mo-0.15 V (0.20 C) deposited metal in the initial state and after plasma hardening described in this study was determined using X-ray diffraction analysis.

The martensite crystal lattice parameter was calculated from the equation based on Bragg's law:

$$= 2 \cdot \sin \theta / \sqrt{h^2 + k^2 + l^2}$$

where λ is the X-ray wavelength (for K radiation $\lambda = 1.936 \text{ \AA}$); d is the lattice spacing of martensite planes (h, k, l planes); h, k, l are the Miller indexes of the diffracted direction; 2θ is the angle of deflection of the crystallographic planes [110] and [220] (the angle was measured accurately). The structure factors were obtained from the experimental diffraction pattern and the result was determined by the extrapolation of parameters

$$d_{110} \text{ and } d_{220} \text{ to } 90^\circ$$

The carbon content in the martensite was calculated based on the interdoublet distance using the calibration graphical chart of $d = f(c)$.

The degree of tetragonality of the martensite lattice was obtained as $c/a = 1 + 0.0467 \cdot d$.

The microdistortions of the crystal lattice were calculated from $\epsilon = \frac{d_{220}}{d_{110}} - 1$, where α is the interaxial angle.

The dislocation density was determined from the following equation: $\rho = 2.4 \cdot \epsilon_{110}^2 \times 10^{16}, \text{ m}^{-2}$.